

# **BALLISTIC PERFORMANCE OF MONOLITHIC CERAMIC BACKED BY S2-GLASS/VINYL ESTER COMPOSITES**

A. Haque, A. Abutalib, K. Rahul, U. K. Vaidya, H. Mahfuz and S. Jeelani

*Center for Advanced Materials  
Tuskegee University  
Tuskegee, Alabama-36088, USA*

**SUMMARY :** This paper investigates the high velocity impact response of an alumina ceramic tile bonded to a S2-glass/vinyl ester composite that is of interest in armor vehicle applications. The ballistic limit, residual velocity, energy dissipation and the penetration mechanism of various thicknesses of the two component composite system is compared. The thickness of both the ceramic tile and the backing plate is varied in order to obtain different areal density of the integral armor. An optimal thickness ratio and areal density for both the components is determined to obtain the maximum ballistic limit of this two-component system. The purpose of this optimization is to determine a ratio of ceramic-to-composite backing plate thickness which will provide a specified level of protection at minimum weight. The energy dissipation and the ballistic limit obtained experimentally is compared with an existing analytical model developed for a two component armor system. This model is originally developed for a ceramic bonded with metal structure and showed reasonable correlation with experimental results. In most of the cases the model is applied for cylindro-conical projectiles. This work investigates the validity of the model for fragment simulating projectile, in which case the impact surface of the projectile is flat rectangular shape with slanted edges. The extent of ballistic impact damage and penetration mechanisms are determined through ultrasonic C-scan and microscopic examinations. A numerical scheme is adopted to simulate the ballistic response of both the single and two component composite system using a three-dimensional (3-D) finite element analysis. Both the composite target plate and the projectile with boundary conditions similar to the impact tests are modeled using eight node-solid brick element. The target plates are impacted at different velocities and the displacement and the velocity component of the projectile as a function of time are analyzed and compared with the experimental results.

**KEYWORDS :** Composite Armor, Ballistic Impact, Perforation Mechanisms, Optimization

## **INTRODUCTION**

The recent development in armor design is focussed on achieving more efficient protection against enhanced threat levels of impact. Steel has been used as a traditional armor material for several years because of its superior ballistic properties. The demand for achieving lighter armor, and yet exhibiting better performance, led the way for developing new materials as alternative candidates. Such demand is increased due to present interests toward using armor in bulletproof vests, helmets, infantry fighting vehicles and army tanks. The concept of light weight armor emphasizes the use of non metallic materials such as ceramic and polymer reinforced composites. High strain fibers (glass, kevlar and spectra) with a ductile resin matrix are being

widely used for body armors particularly in helmets and vests. Many investigators have studied the ballistic performance of these polymer matrix composites (PMCs) against different threat levels [1-3]. It appears that PMCs are suitable to defeat small caliber balls and fragments but their performance is poor when it comes to defeat armor piercing projectiles. Ceramics possess two characteristics such as low density and high hardness, which makes them attractive in armor applications. In most cases, ceramic is used as an added component to the structural part to enhance the ballistic performance of an integral armor. The design of complex armor system for improved ballistic performance and high structural integrity emphasizes the use of hard ceramic materials backed by ductile aluminum alloy or high strain fiber reinforced polymer composites. Such a two component composite armor is advantageous over a single component in resisting high stress levels with minimum deformation provided by the hard ceramic face material and simultaneously sustaining high tensile failure strain supported by the composite backing plate. This combined material characteristic of the integrated system possesses the capacity to enhance both the ballistic and structural performance of the armor.

Understanding the penetration and perforation mechanisms of ceramic backed polymer composites and identifying the relevant control parameters for optimum ballistic performance are very important for armor design. The earlier work of Wilkins [4] studied the ballistic performance of ceramic tiles backed by aluminum plates against 7.62 mm projectile and later on significant research has been carried out to understand the ballistic performance of ceramics with metallic backing for different fragments and projectiles. The key parameters that are most important in studying the ballistic performance of an armor are ballistic limit, energy absorbed and the deformation behavior, which in turn depends on the characteristics of the projectiles, targets and constraints applied to the target objects. These characteristics primarily represent the physical and mechanical properties, geometric parameters and loading conditions that are applied to both the projectile and target object. The study related to high velocity impact mostly focuses on the experimental observations, analytical models and numerical simulations of the impact response. The work in all these areas particularly for ceramic bonded with polymer composite armor materials is very limited [5-8]. In this study the high velocity impact response of alumina ceramic backed by S2-glass/vinyl ester composite laminate has been studied. The experimental observations are compared with an analytical model and finite element analysis. The fracture behavior of both the ceramics and the composites, deformation behavior of the projectiles and targets and the damaged areas are investigated and reported in this paper.

## **EXPERIMENTAL WORK**

### **Specimen Fabrication**

The composite panels were fabricated using S2-glass twill weave fabric and vinyl ester resin through Vacuum Assisted Resin Infusion Process (VARIP). A center injection and two side-ejection resin infusion process was adopted for making the laminate. The laminates of six thicknesses ( $h_2$ ) were fabricated and afterwards each panel was bonded to three thicknesses ( $h_1$ ) of alumina ceramic tiles. The bonding of alumina tiles with composite backing plate was performed using an epoxy adhesive. A total of eighteen samples with different thicknesses of ceramic tiles and the composite backing plates were manufactured to attain variable areal densities.

## Ballistic Test Procedure

The impact tests were performed using a gas gun test set up with 0.5 caliber fragment simulating projectiles (FSP). A schematic of the complete gas-gun test condition is shown in Figure 1. A sabot stripper plate was used to separate the projectile from the sabot, before hitting the target.

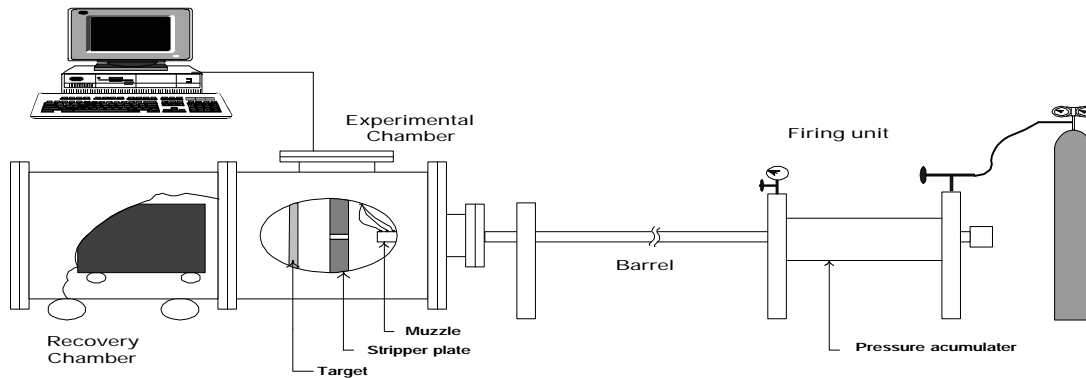


Fig. 1 A schematic of complete gas gun test set-up

The impact performance of the target materials was characterized through the determination of projectile velocity prior to penetration and after the perforation of the target object. Such measurements were carried out using magnetic sensors in two locations. One set of sensor was attached at the end of the muzzle in front of the target plate to measure the striking velocity and other set was placed at location behind the target plate to measure the residual velocity. The velocities of the projectile were determined from the measurement of transit time over fixed distance between the individual magnetic sensors. Hence, impact energy and residual energy calculations were made from the measured striking ( $V_s$ ) and residual ( $V_r$ ) velocity. The ballistic limit ( $V_{BL}$ ) was determined from the simple relationship  $\frac{1}{2} m_p V_{BL}^2 = \frac{1}{2} m_p V_s^2 - \frac{1}{2} m_p V_r^2$ , for  $V_s > V_{BL}$  where  $m_p$  is the mass of the projectile.

## Perforation Mechanisms and Damage Evaluation

Damage evaluation and assessment of failure modes of the projectiles and the target objects were carried out to enhance the understanding of the dynamic deformation process. Such measurements provided information pertaining to the principle dimensions of the impact damage zone, such as entrance and exit areas for perforation, damage profile (shape, size and location) as well as the final length, diameter, and mass of the projectile and other fragments. The perforation mechanism and damage of all the impacted samples were identified through ultrasonic C-scan, optical and scanning electron microscopic examinations.

## ANALYTICAL PREDICTION

The ballistic limit and the absorbed energy were predicted by means of an analytical model developed by Florence for a two component armor system [9]. This model considers that a short

cylindrical rod while impacting a hard material forms a cone of fractured materials which eventually transmits all the impacting energy to a ductile backing plate. The backing plate is assumed as a circular membrane or a plate fixed at the circular boundary and having an initial mass and velocity distribution. The velocity distribution is associated with the fundamental mode of vibration of the circular membrane with a peak value determined by conservation of momentum. Considering the maximum strain failure criterion in the backing plate the ballistic limit velocity of the projectile ( $V_p$ ) for a two component system is given by the following simple equation :

$$V_p = \frac{(\epsilon_f \sigma_s)^{1/2}}{(0.91 f(a) m_p)^{1/2}} \quad (1)$$

where  $\epsilon_f$  is breaking strain of backing plate,  $\sigma_s = \sigma_f h_2$ ,  $\sigma_f$  = ultimate tensile strength of the backing plate,  $h_2$  = backing plate thickness,  $f(a) = m_p / (m_p + (h_1 d_1 + h_2 d_2) \pi a^2) \pi a^2$ ,  $m_p$  = projectile mass,  $h_1$  = hard plate thickness,  $d_1$  = density of hard plate,  $d_2$  = density of backing plate,  $a = a_p + 2 h_1$ ,  $a_p$  = radius of the projectile

## NUMERICAL SIMULATION

The numerical simulation of high velocity impact response was performed using the DYNA-3D finite element code which was developed for analyzing the large deformation dynamic behavior of structures [10]. The main solution methodology in DYNA-3D is based on explicit time integration scheme. It is suitable for problems in which high-rate dynamics or wave propagation effects are important. The explicit time integration scheme is based on the central difference method and the velocities and displacements are updated in each time step. The models for both 0.5 FSP projectile and S2-glass/vinyl ester composite backed ceramic (two component system) were developed by using an eight noded solid brick element. The contact interface between the projectile and the target object uses a surface-to-surface eroding algorithm. One side of the interface is designated as the slave side, and the other side of the interface is designated as master side. Nodes lying in those surfaces are referred to as slave and master nodes, respectively.

## RESULTS AND DISCUSSIONS

### Ballistic Response

Table 1 shows impact test results for ceramic bonded to S2-glass/vinyl ester composite target plates with different areal densities. It is to be noted that the test results of all eighteen samples are not included in Table 1. This is due to the fact that complete penetration of all the test specimens were not achieved with the available striking velocity range of the gas-gun. The test results show complete penetration for only four specimens out of nine test samples. In some cases the projectile either rebounded or resided within the target object. It was found that the level of the striking velocity influences the energy absorbed, which in turn affects the ballistic limit ( $V_{BL}$ ). This represents some disadvantages of determining the ballistic limit from the absorbed energy, although it requires less number of tests in comparison to  $V_{50}$  measurements. As a result it is recommended to apply the same range of striking velocity ( $V_s$ ) for comparison of absorbed energy for different specimens.

Table 1. Ballistic impact test data for ceramic-composite system

No.	$h_1$ (mm)	$h_2$ (mm)	$h_1/h_2$	$A_D$ (Kg/m <sup>2</sup> )	$V_s$ (m/s)	$V_r$ (m/s)	$E_{ab}$ (Joules)	$V_{BL}$ (m/s)
1	6.35	3.86	1.65	29.13	554.3	211.5	1745.7	512.4
2	6.35	6.98	0.91	34.72	752	274	3261.3	700.3
3	6.35	9.27	0.69	38.82	889	317	4587.0	830.5
4	6.35	12.27	0.52	44.18	918.3	233	5246.8	888.2
5	6.35	15.14	0.42	49.32	919.0	Resided	5630.97	
6	6.35	12.27	0.52	61.04	948.2	Resided	5990.93	888.2
7	12.7	3.86	3.29	51.36	814	Rebounded	-	-
8	12.7	15.14	0.42	71.55	920.3	Rebounded	-	-
9	12.7	21.44	0.59	82.82	948.92	Rebounded	-	-

$V_s$ : striking velocity  
 $V_{BL} = (V_s^2 - V_r^2)^{0.5}$ , Ballistic limit  
 $E_{ab} = 1/2 m_p (V_s^2 - V_r^2)$ , Energy absorbed  
 $V_r$ : residual velocity

Table 2 shows the theoretical prediction of the absorbed energy and the ballistic limit for all the test specimens where complete penetration took place. The ballistic limit  $V_p$  in Table 2 was determined from Equ. 1. The predicted absorbed energy was determined from  $1/2 m_p (V_s^2 - V_{rth}^2)$  in which  $V_{rth}$  was predicted from  $V_s - V_p$  based on conservation of momentum. The predicted striking velocity ( $V_s$ ) was considered to be same in magnitude as used in the impact tests.

Table 2 Theoretical prediction of ballistic limit and absorbed energy

$h_1$ (mm)	$h_2$ (mm)	$h_1/h_2$	$A_D$ (Kg/m <sup>2</sup> )	$V_p$ (m/s)	$V_{rth}$ (m/s)	$E_{ab}$ (Joules)	$V_{BL}$ (m/s)
6.35	3.86	1.65	29.13	161.4	392.9	1016.8	391.0
6.35	6.98	0.91	34.72	231.5	520.5	1958.7	542.7
6.35	9.27	0.69	38.82	287.3	610.7	2775.2	646.0
6.35	12.27	0.52	44.18	336.7	581.6	3358.7	710.7

$V_{rth} = (V_s - V_p)$ ,  $V_{BL} = (V_s^2 - V_{rth}^2)^{1/2}$   
 $E_{ab} = 1/2 m_p (V_s^2 - V_{rth}^2)$

It is to be noted that the absorbed energy predicted from  $1/2 m V_p^2$  shows significant difference as compared to the experimental absorbed energy. The predicted ballistic limit,  $V_{BL}$  in Table 2 was determined from the term  $(V_s^2 - V_{rth}^2)^{1/2}$  which showed much less discrepancy with the experimental ballistic limit in comparison to  $V_p$ , as suggested by the Florence model. Such modification was considered because the experimental ballistic limit was determined on the basis of conservation of energy and the Florence model is based on conservation of momentum. Figures 2 and 3 show a comparison of the experimental and theoretical ballistic performance and absorbed energy as a function of areal density for two component armor system. The results clearly show the trend of increasing ballistic limit and absorbed energy with the increase in areal density for all the cases.

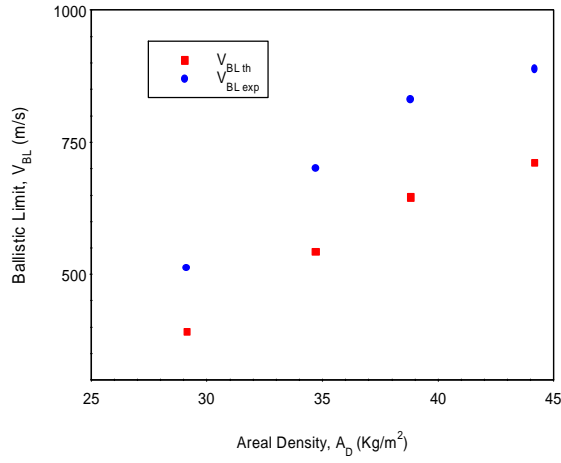


Fig. 2 Ballistic limit vs. areal density

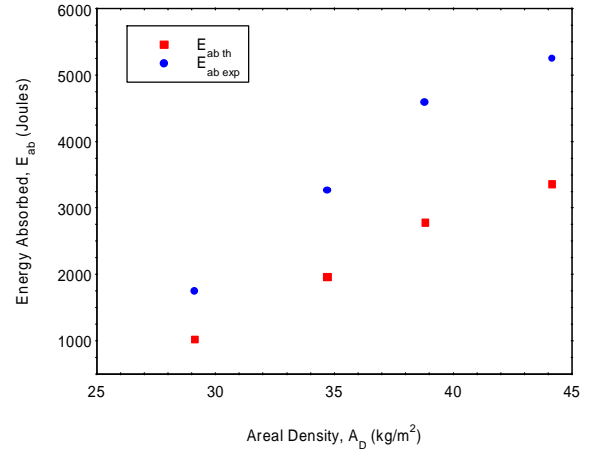


Fig. 3 Absorbed energy vs. areal density

The experimental ballistic limit and the absorbed energy are shown to be approximately 22 % and 44 % higher than the predicted quantities. The discrepancy between the experimental and predicted results is due to the fact that the energy absorbed in deforming the projectile and fracturing the ceramic is not considered in the analytical model. Further work is necessary to improve the model considering the above factors. Figure 4 shows optimization curves for the predicted ballistic limit,  $V_{BL}$  as a function of thickness ratio and areal density. Some experimental data is also shown in Fig. 4 for a comparison with the predicted ballistic limit,  $V_{BL}$ . It is found that a thickness ratio of approximately 1.25 is the optimum level to achieve the highest ballistic limit for a S2-glass/vinyl ester composite backed alumina ceramic armor. Ballistic limit is shown to increase at a faster rate up to a thickness ratio,  $h_1/h_2 = 0.75$  and then a decreasing trend is observed beyond  $h_1/h_2 = 1.25$ . An increased ballistic limit is seen with an increased areal density for all the thickness ratios,  $h_1/h_2$  considered in this study.

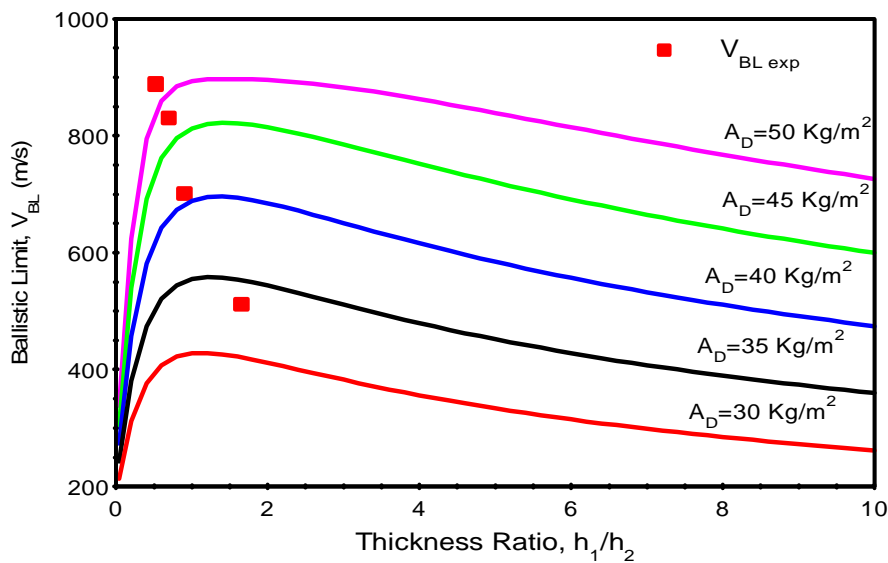


Fig. 4. Ballistic limit vs. thickness ratio, ( $h_1/h_2$ ) and areal density ( $A_d$ )

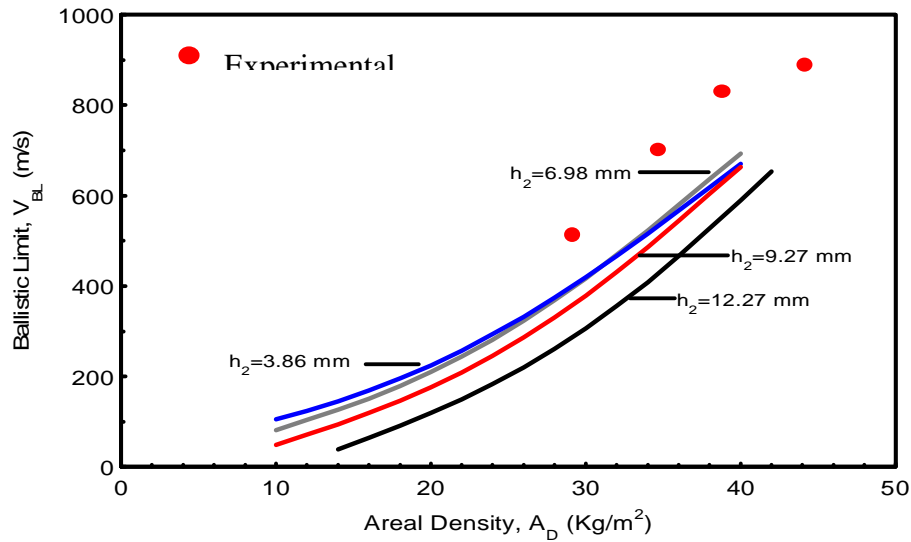
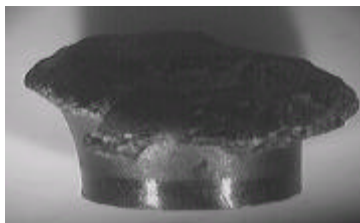


Fig. 5 Dependence of ballistic limit on areal density and backing plate thickness

Figure 5 shows the dependence of ballistic limit on the areal density and the thickness of the backing plate. The ballistic limit is seen to increase as the backing plate thickness reduces, while the areal density of the target plate remains constant. Such a trend is very prominent when the specimens having  $h_2 = 3.86$  mm and 12.27 mm are compared.

Figure 6 shows the ballistic impact fracture mechanism for both the projectile and the specimen no. 3 in Table 1. The impact velocity of the projectile was 889 m/s and the residual velocity after impact was recorded to be 317 m/s.



Projectile



Ceramic facing



Impact-face



Back-face

Fig. 6. Penetration and perforation mechanism of the composite backed ceramic target object and the deformation behavior of the projectile

The deformed projectile is appeared like a mushroom at the impact face with a decrease in its overall length. The mushroom like appearance is primarily due to the large compressive stresses on the projectile, as it strikes the hard ceramic. The fractured surface of the ceramic tile was almost conical in shape with a diameter of 6 cm at the back face and 4.5 cm at the impact face. The modes of fracture were predominantly tensile and bending with radial cracks propagated towards the corners and edges of the ceramic tile. The ceramic tile was totally separated from the backing plate after the impact with significant amount of spalled ceramic fragments. Localized resin and fiber crushing were observed at the impact face of the composite backing plate. Multiple delaminations of conical shape were formed within the backing plate and the delaminations initiated at the location where the incident and reflected waves meet during wave propagation. The diameters of the damaged zones at the impact and rear sides of the backing plate were 4.3 cm and 15.25 cm respectively.

Figure 7 shows the numerical simulation of the projectile velocity and the displacement during the perforation of composite backing plate without ceramic tile. The displacement vs. time plot in Fig. 7 shows that the tip of the projectile reaches the back face of the target plate at time of 10  $\mu$ sec and during this time period the velocity of the projectile is shown to decrease at a faster rate. The displacement at 10  $\mu$ sec is shown to be 7 mm which is approximately equal to thickness of the specimen (6.98 mm). It is also shown that the rear side of the projectile emerges from of the specimen after it travels approximately a distance of 2.35 cm at a time period of 40  $\mu$ sec. This distance is very close to the sum of the specimen thickness (0.69 cm) and the projectile length (1.48 cm).

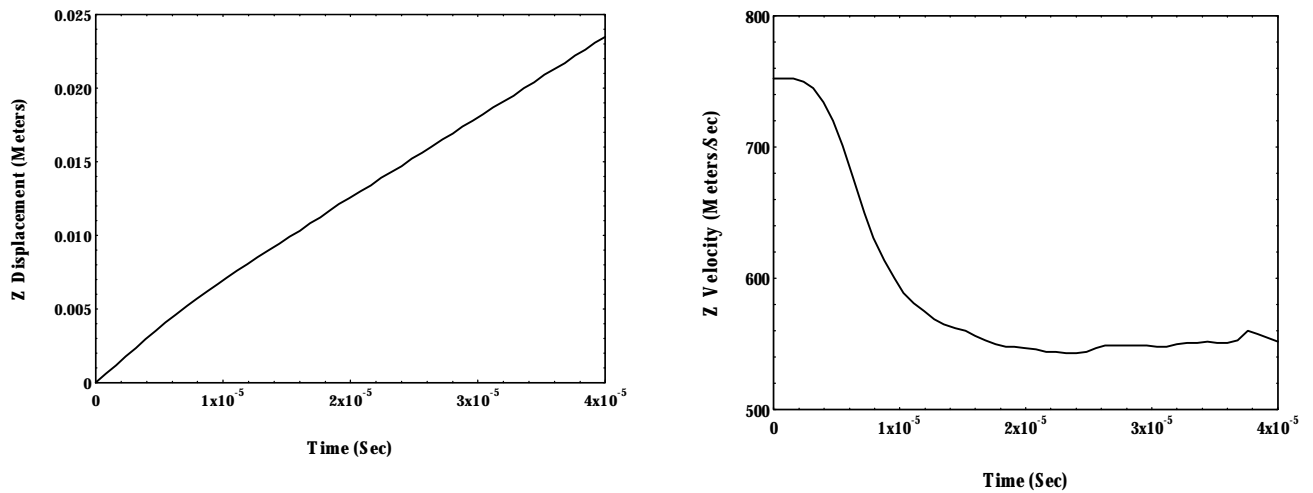


Fig. 7 Numerical simulation of the displacement and velocity of the projectile during perforation of S2-glass/ vinyl ester composites (thickness : 6.98 mm)

Figure 8 shows the numerical simulation of the velocity and displacement profiles of the projectile during the penetration and perforation of a two component armor system (specimen # 2 in Table 2). The total thickness ( $h_1 + h_2 = 6.35 \text{ mm} + 6.98 \text{ mm}$ ) of this specimen was 13.33 mm. The numerical simulation shows that the penetration of the backing plate started at approximately 9  $\mu$ sec (time required to travel 6.35 mm) and the projectile tip reached the back face of the S2-glass/vinyl ester laminate at 18  $\mu$  sec (time required to travel 13.33 mm). During



this penetration process (duration : 18  $\mu$ sec ) the velocity reduced at a faster rate and after the projectile tip reached the backing plate (perforation stage), the velocity dropped at a slower rate. The experimental residual velocity for this specimen is shown to be 274 m/sec against the numerical simulation of 305 m/sec. The residual velocity in the numerical simulation was considered at a time interval of 90  $\mu$  sec and during this time interval the projectile traveled a distance of 36 mm as shown in Fig. 8. This should be approximately close to the target thickness (13.33 mm), plus the deformed projectile length (12.20 mm), added to the deflection of the target object (5 mm). The deflection considered in this calculation was static deflection which was measured after the impact. This shows reasonable correlation between the experimental and numerical simulation.

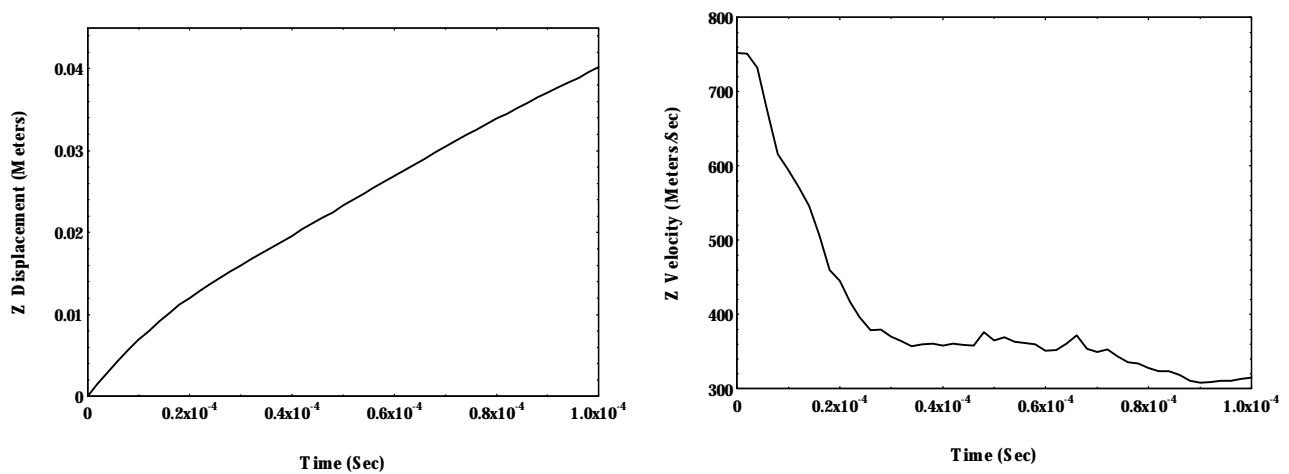


Fig. 8 Numerical Simulation of the displacement and velocity of the projectile during perforation of ceramic backed by S2-glass/ vinyl ester composite laminate (thickness : 13.35 mm )

## CONCLUSIONS

The following conclusions are drawn from the results of this investigation:

1. The experimental ballistic limit and the absorbed energy are seen to be approximately 22 % and 44 % higher than the theoretically predicted quantities. This discrepancy possibly occurred from ignoring the energy dissipated in deforming the projectile and fracturing the ceramic tile in the theoretical analysis.
2. The ballistic limit of S2-glass/vinyl ester composite backed ceramic armor is seen to increase rapidly up to a thickness ratio  $h_1/h_2 = 0.75$ , and the optimum ballistic limit, found to lie between a thickness ratio of 1 to 1.25. At constant areal density the ballistic limit is seen to be higher for a thin backing plate.
3. The projectile deformed to a mushroom shape under high compressive loading. Conical fracture was observed in the ceramic tiles with cracks propagating outwards in radial direction. The composite backing plate is seen to develop severe matrix cracking and fiber fracture under shear and tensile loads arising from the impact.

4. The numerical simulation of the velocity and displacement of the projectile as a function of time shows reasonable agreement with the experimental observations.
5. Future work is necessary to improve the theoretical model and the numerical simulation of two component armor system. The ballistic limit determined from the absorbed energy needs to be compared with  $V_{50}$  measurements.

## **REFERENCES**

1. Howlett, S. And Greaves, L., "The Penetration Behavior of Glass Fiber Reinforced Plastic Materials", Proceedings of ICCM-10, Whistler, B.C., Canada, August 1995
2. Bless, S. J. and Hartman, D. R. , " Ballistic Penetration of S-2 Glass Laminates" 21<sup>st</sup> International SAMPE Technical Conference, September 25-28, 1989
3. Haque, A. , Vaidya, U. K., Kulkarni, M., Kulkarni, R., "Influence of Polycarbonate on the Ballistic Performance of S2-Glass/Epoxy Composites", Proceedings of the International Conference on Advanced Composites 98, Hurghada, Egypt, December 15-18, 1998, pp. 17-27.
4. Wilkins, M. L., Landingham, R. L. & Honodel, C. A. Fifth Progress Report of Light Armor Program, Lawrence Radiation Lab. Rept. UCRL-50980, 1971
5. Hetherington, J. G. " The Optimization of Two Component Composite Armours", Int. J. Impact Engineering, Vol.12, No.3, 1992, pp. 409-414
6. Wang, B. and Lu, G., " On the Optimization of Two-component Plates Against Ballistic Impact" Journal of Materials Processing Technology 57 (1996) pp. 141-145
7. Hetherington, J. G. and Rajagopalan, " An Investigation into the Energy Absorbed during Ballistic Perforation of Composite Armors" Int. J. Impact Engineering, Vol. 11, No1. Pp. 33-40, 1991
8. Horsfall, I. And Buckley, "The Effect of Through-Thickness Cracks on the Ballistic Performance of Ceramic Armor Systems" Int. J. Impact Engineering, Vol 18, No.3, 1996, pp. 309-318
9. Florence, A. L., " Interaction of Projectiles and Composite Armor", Part II, Stanford Research Institute, Menlo Park, California 94025
10. John O. Hallquist, LS-DYNA3D Theoretical Manual, Livermore Software Technology Corporation, Livermore, Ca 94550

